ChemComm

Accepted Manuscript

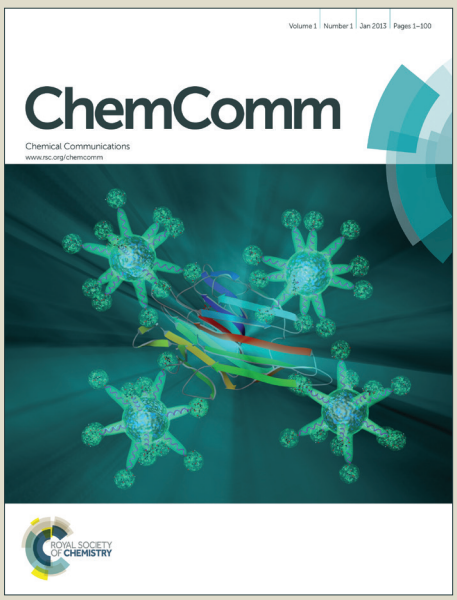

ROYAL SOCIETY OF CHEMISTRY

www.rsc.org/chemcomm

Journal Name

RSCPublishing

COMMUNICATION

High aspect ratio, processable coordination polymer gel nanotubes based on an AIE-active LMWG with tunable emission

Cite this: DOI: 10.1039/x0xx00000x

Received 00th January 2012,
Accepted 00th January 2012

DOI: 10.1039/x0xx00000x

www.rsc.org/

Venkata M Suresh, Anangsha De and Tapas Kumar Maji*

A new TPE based low molecular weight gelator (LMWG) which displays both AIE and MCIE phenomena in gel state have been synthesized. LMWG self-assembles to form 1D nanofibers which undergo morphology transformation to coordination polymer gel (CPG) nanotubes on metal ion coordination. CPG shows enhanced mechanical stability along with tunable emission properties.

Self-assembly of π-conjugated low molecular weight gelators (LMWGs) having hydrophobic and hydrophilic segments through non-covalent interactions has been an attractive strategy in designing artificial nanostructures such as fibers, vesicles, rings, ribbons and tubes.[1] Particularly, one dimensional (1D) nanostructures with fibrillar or tubular morphologies of π-conjugated chromophores are important for optoelectronic materials, as they provide feasible pathway for efficient energy migration or charge transport, and several such systems based on organic LMWG have been documented.[2] However, aggregation caused luminescence quenching (ACQ) in π-stacked chromophoric organic assemblies and their thermal/mechanical stability have been a limiting issue for practical applications in organic light emitting diodes and luminescent sensors. The discovery of aggregation induced emission (AIE) phenomena for unique luminescence features of tetraphenylethene (TPE) in solid aggregates has provided opportunity in overcoming ACQ effect.[3] The restricted rotation of phenyl rings through intermolecular Ph…H and Ph…Ph stacking interactions in TPE dramatically enhances the emission and quantum yields compared to solutions and offer potential applications in biological sensors, organic light emitting diodes (OLEDs) and field effect transistors (FETs).[4] Nevertheless, the restricted rotation of phenyl moieties and population of radiative states, thus intense emission has also been achieved either by integrating the TPE into metal-organic frameworks (MOFs) structure through metal ion coordination called matrix coordination induced emission (MCIE) or into conjugated microporous polymers (CMPs) by covalent linkage called framework induced emission (FIE).[5] Despite of its integration in 3D porous frameworks, complete restriction of phenyl ring rotation is not achieved due to very low energy barrier of phenyl rotation,[6] which causes partial quenching of fluorescence of the framework. Therefore, we envisioned to design a new amide functionalized LMWG based on a TPE derivative (AIE active) with terminal terpyridine (TPY) units which would self-assemble via intermolecular H-bonding (Scheme 1) and metal coordination to form a three dimensional coordination polymer gel, where both AIE and MCIE phenomena can be observed. Thus soft CPG with enhanced and tunable emission can be realized.[7] In contrast to metal-organic gels derived from discrete metal complexes,[8] coordination polymer gels (CPGs) based on polydentate π-conjugated LMWGs are unique due to their long range structural ordering of the chromophores based on nanoscale periodicity of inorganic components. In addition, high thermal/mechanical stability and functions related to metal-ion such as magnetism, luminescence and catalytic activity can be comprehended.[9] Further, the metal ligand bonds are amenable to reaction parameters thereby modular nanoscale materials with versatile morphologies can be perceived.[10] Although organic assemblies of TPE derivatives is well studied, their coordination assisted self-assembly toward CPG with variable nano architectures and photophysical properties is yet to be explored.[11] Here in, we aim to study the effect of metal-coordination on the secondary structure of self-assembly thus nanomorphologies and their luminescence properties arising from combination of AIE and MCIE phenomena of tetrakis(4-carboxyphenylethene) acid tetrakis-{[3-([2,2′:6,2″]terpyridine-4′-ylamino)-propyl]-amide} (**L**) in corresponding gel state.

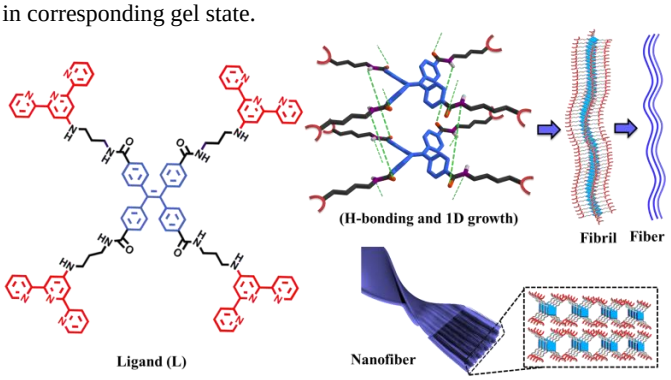

Scheme 1. Schematic representation of self-assembly of **L** through H-bonding between amide groups and formation of 1D nanostructures.

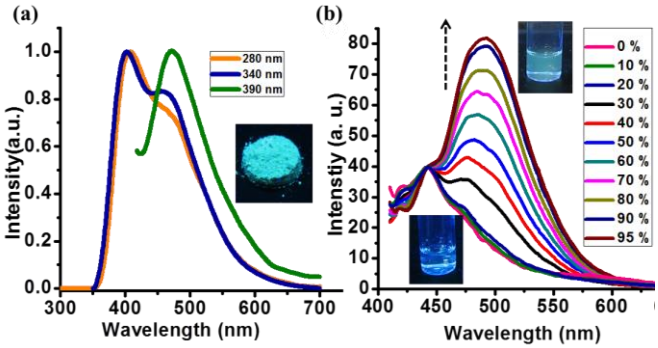

Fig. 1 Aggregation induced emission behaviour of **L** in solid state: (a) Emission of L in solid state at different excitation wavelengths (inset: Image of **L** solid powder under UV light). (b) Gradual changes in emission spectra of **L** (10^{-3} M) in methanol on increasing the volume fraction of H_2O from 0-95 % (Normalized at 440 nm).

LMWG, **L** has been synthesized by reacting amine derivative of terpyridine with TPE acid chloride in tetrahydrofuran (THF) at 0°C conditions (Fig. S1, see: †ESI for details). Formation of **L** is confirmed by ^{1}H-NMR, HRMS (Fig. S2, †ESI) and Fourier transform infrared spectroscopy (FTIR). **L** shows band at 1643 cm^{-1} and 3420 cm^{-1} corresponding to ν(>C=O) and ν(N-H) stretching vibrations confirming the formation of amide bond (Fig. S3). Absorbance spectra of **L** in solid state (Fig. S4) showed two major bands at 280 nm and 350 nm corresponding to π-π* transition of TPY and TPE groups respectively,(Fig S5, S6) suggesting the presence of two individual chromophoric units in **L**.[5a,9g] Excitation at 280 nm showed main emission at 410 nm ascribed to the TPY core while excitation at 390 nm showed main emission at 480 nm originating from TPE core of **L** due to the AIE phenomena operating in solid state (Fig. 1a).[3a] Excitation of dilute solution of **L** in MeOH, DMF, EtOH at 280, 340 and 380 nm showed emission at 410 nm and only weak emission at 480 nm due to fast phenyl rotations of TPE segment (Fig. S7-S10).To further study the AIE of **L**, emission studies were carried out in binary mixture of MeOH/H_2O. Dilute solution of **L** (10^{-3} M) upon excitation at 380 nm showed very weak emission at 480 nm in pure methanol that is at 0 % H_2O. However, on increasing the H_2O content from 0-95 % by volume fraction, gradual enhancement in emission intensity at 480 nm is observed (Fig. 1b). This emission enhancement at 480 nm is ascribed to the formation of **L** aggregates on addition of H_2O. These results are explained on the basis of AIE effect of TPE core of **L**. In dilute solutions (10^{-3} M); the phenyl ring rotations of TPE segment are exclusively significant which opens up the non-radiative decay channels thereby quenching the emission from TPE core. However, on addition of H_2O, aggregation of **L** occurs where the Ph…Ph or Ph…H intermolecular interactions greatly reduce phenyl rotation of TPE and open up radiative channels resulting in enhanced emission.

Heating and cooling of **L** (7×10^{-3} M) in $CHCl_3$/THF (1:2) mixture results in formation of a stable gel and is confirmed by inversion test method (Fig. 2a, †ESI). Gel converts reversibly into viscous liquid on shaking and to gel on standing at room temperature. As shown in Scheme 1, it is expected that **L** self-assembles through intermolecular H-bonding interaction between amide functional groups and form 1D nanostructures. Presence of intermolecular H-bonding in xerogel is evident from FTIR studies, **L** xerogel show bands at 1632 cm^{-1} and 3399 cm^{-1} corresponding to ν(>C=O) and ν(N-H) stretching vibrations respectively which are shifted to lower regions in comparison to assynthesized ligand suggesting the presence of intermolecular H-bonding (Fig. S3). On

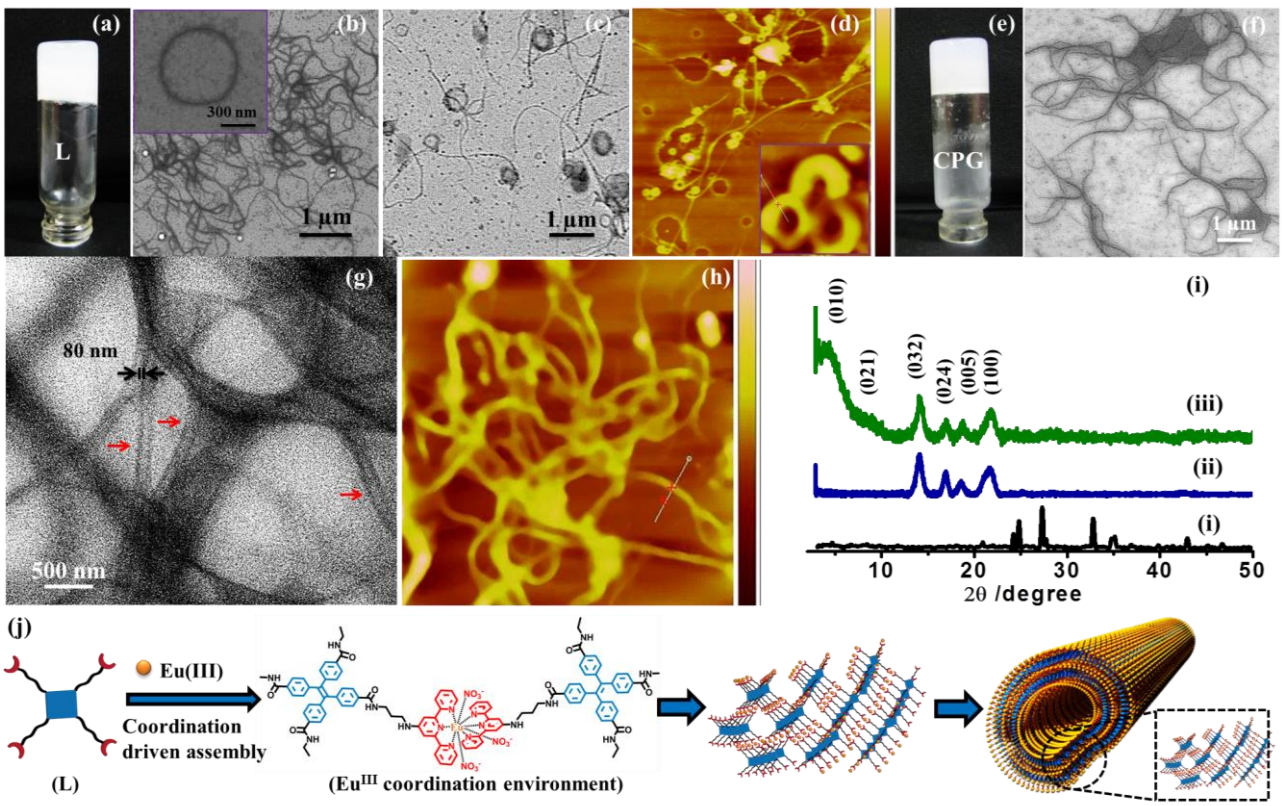

Fig. 2 (a) Day light image of **L** gel, (b) FESEM image of **L** gel fibers, Inset; single nanoring of **L** gel, (c) TEM image showing presence of nanofibers and coiling of nanofibers toward ring formation in **L** gel and (d) AFM images of nanorings and nanofibers of **L** gel. (e) Day light image of CPG, (f) FESEM image, (g) TEM images showing the nanotubular structures of CPG and (h) AFM image of nanotubes. (i) PXRD at different state: solid ligand powder (i), **L** xerogel(ii), and CPG(iii), (j) Schematic showing the proposed self-assembly of CPG to form nanotubular structure.

the other hand, field emission scanning electron microscopy (FESEM) of **L** xerogel shows formation of micrometer long nanofibers of diameter 90-100 nm along with coiled nanostructures or rings with varied diameters (Fig. 2b, Inset and Fig. S11). Further, transmission electron microscopy (TEM) shows formation of nanofibers and coiled nanostructures (Fig. 2c, S12) of dimensions consistent with SEM. These results suggest that the ring formation indeed happen *via* coiling of high aspect ratio nanofibers during gelation process. AFM cross-sectional analysis (Fig. 2d, S13) of xerogel of **L** shows nanofibers and coiled nanostructures of diameter 100±10 nm which is consistent with SEM, TEM results and corresponding height of the fibers were found to be 21±1 nm (Fig. S14). The packing in gel is further supported X-ray diffraction (XRD) measurements of **L** xerogel; diffraction peak at 21.7° with *d*-spacing value of 4.0 Å suggests weak π-π interactions between TPE cores of **L**.[12a] These results clearly suggest that **L** indeed self-assembles through H-bonding interactions and form 1D nanostructures such as nanofibers and coiled nanostructures.

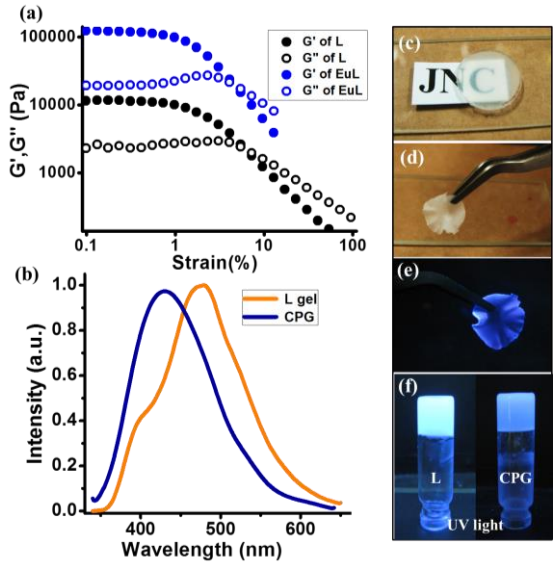

Fig. 3 (a) Oscillatory strain measurements of **L** gel (black) and CPG (blue), filled and open circles indicate storage and loss modulus respectively. (b) Photoluminescence spectra of **L** gel (orange) and CPG (blue), (c), (d), (e) Formation of transparent and stable films of CPG showing its easy processability and stability. (f) Images of **L** gel and CPG under UV light.

L contains four TPY units connected to phenyls of TPE through flexible alkyl chain and amide functionality. Self-assembly of **L** through metal ion coordination forms a 3D coordination polymer. Interaction of Eu(III) ion with **L** is studied by absorption spectra by titrating against $Eu(NO_3)_3{\cdot}6H_2O$ in methanol (Fig. S15, see †ESI for details). **L**/$Eu(NO_3)_3{\cdot}6H_2O$, (1:2 eq) in $CHCl_3$/THF (1:2) results in turbid solution which on further heating and cooling leads immediate gel formation (see †ESI for details), which is confirmed by inversion test method(Fig. 2e). Presence of Eu(III) ion in the CPG is confirmed by energy dispersive X-ray analysis (EDAX) (Fig. S16). Presence of intermolecular H-bonding in CPG is evident from FTIR with lowering in ν(>C=O) and ν(N-H) stretching frequencies similar to **L** xerogel. Further, a strong peak at 1382 cm^{-1} is corresponding to ν(N-O) stretching vibration, indicating the presence of coordinated nitrate ion in CPG (Fig. S3). These results clearly suggest definite coordination of Eu(III) ion to the TPY units of **L**, and the possible coordination environment of metal ion is depicted in Fig. S17. FESEM of xerogel shows 1D nanostructures of micron length with diameter of 160-200 nm (Fig. 2f, S18). While, TEM at high magnification show formation of high aspect ratio nanotubes with uniformly spaced dark lines separated by bright core. The wall thickness is observed to be 80-100 nm with several micron length (Fig. 2g, S19, 20). Height of the nanotubes calculated from the AFM cross-sectional analysis is found to be 40±2 nm (Fig. 2h & S21, S22). Structural ordering by metal ion binding is further evident by XRD measurements. Interestingly, diffraction pattern of CPG at higher angle is observed to be comparable with **L** gel suggesting similarity in the primary structure of the self-assembled gels. However, an additional diffraction peak at 4.0° (*d*-spacing: 21.9 Å) is observed in case of CPG and this *d*-spacing value closely matches with calculated distance between two Eu(III) centers bridged by **L** (Fig. S23). Indexing diffraction pattern of CPG (Fig. 2i) using CRYSFIRE powder indexing system using Taup (TP) program (see †ESI Table 1) suggest an orthorhombic phase for CPG, where a = 4.08574 Å, b = 22.3266 Å, c = 23.6498 Å and V= 2157.35 ($Å^3$). Low angle diffraction peak at 4.0° is assigned to (010) plane, which corresponding periodicity along the metal centers (Fig. S24) and peak at 21.7° (d = 4 Å) correlates to the molecular stacking of TPE units.[12a] Based on the preceding results, a proposed model for self-assembly of CPG is envisaged (Fig. 2j). Initially, **L** self-assembles through intermolecular H-bonding of amide groups and forms 1D nanostructure leaving free TPY moieties on the surface which are bridged by the metal ions and extend the self-assembly into an infinite 3D coordination polymeric structure. It is believed that the TPY units around Eu(III) ion arranges themselves in an orthogonal orientation in order to reduce steric repulsion and results in bending of nanostructures to form nanotubular morphology.

To investigate the effect of metal ion binding on mechanical properties, we have performed oscillatory strain sweep measurements on organogel and CPG at a frequency of 1 rad/sec. As seen in Fig. 3a, storage modulus (G′) for both the gels is larger than the loss modulus (G″) for $\gamma < 5$ % thereby suggesting elastic nature of the gels. For both gels G′>G″ at smaller strains and with increasing strain G′ decreases with a simultaneous rise in G″ indicating the transition of gels from viscoelastic solid to a viscoelastic liquid region. Further, the presence of peak in G″ indicates soft glassy behaviour of the gels. It is clear from Fig. 3a, for all strains <4 %, G′ and G″ are greater than 20 MPa for both gels, such features were also observed in literature.[13] Interestingly, we observed that G′ of CPG is at least an order of magnitude larger than G′ of **L** gel suggesting enhanced rigidity of CPG over **L** gel. The higher rigidity of CPG can be visualized from interconnected 3D network like structure present in CPG due to metal-coordination.

We have studied in details the photophysical properties of **L**-gel and the effect of metal coordination in emission properties of **L**. **L** xerogel shows broad absorption band with λ_{max} = 340 nm, while the CPG shows 10 nm blue shifted absorption band with λ_{max} = 330 nm, this blue shift in the absorbance spectra of CPG can be attributed to the decrease in the planarization of TPE moiety or more twisting of phenyl moieties of TPE on metal coordination in contrast to **L** xerogel (Fig. S24). **L** gel shows strong cyan emission when excited at 340 nm with maxima at 460 nm, while CPG shows strong blue emission with maxima at 435 nm (λ_{ex} = 330 nm) with a significant hypsochromic shift of 25 nm with respect to the **L** gel (Fig. 3b, 3f). In general, the enhanced emission intensity of AIE chromophores is dependent on extent of aggregation, and emission maxima strongly depends on extent of planarization or conjugation of TPE phenyls in aggregated state. When **L** self-assembles through H-bonding the rotation of phenyls is greatly inhibited due to effective Ph…Ph interactions between the stacked TPE units of **L** which results in opening of radiative decay pathways and thus AIE is realized. On the other hand, when Eu(III) binds to **L** in case of CPG, the emission properties can be attributed to the combined effect of MCIE and

AIE. The MCIE has been observed in TPE-tetracarboxylate based MOF by the restriction of the TPE phenyl rotation through metal coordination.[5a] In addition, the three dimensional coordination polymer network like structure of CPG where the two TPY units position orthogonally decreases effective close packing of **L** TPE units leading to decreased planarization of TPE phenyls in CPG in comparison to **L** gel. Thus metal coordination of **L** decreases planarization and results in blue emission for CPG.[12b] Resembling **L** solid powder, excitation of **L** gel at 280 nm showed two bands at 420 nm corresponding to TPY and 460 nm corresponding to TPE (Fig. S25), however the emission of TPY is slightly red shifted, this may be due to the π-π interaction between TPY units in **L** gel that involved in 1D ordered packing. Excitation at 340 and 390 nm showed main emission at 460 nm corresponding to TPE segment similar to **L** solid powder. Time resolved fluorescence life time showed life time of 0.9 (τ_1), 3.1 ns (τ_2) and 0.8(τ_1), 3.2 ns(τ_2) for **L** solid powder and L gel respectively and corresponding quantum yields are found to be 4.3 %, 2.6 % upon excitation at 380 nm respectively (Fig. S26).Solution processibility is key for several practical application or device fabrication of these gels. In spite of their rigidity, CPG gel can be easily transferred onto solid substrates with gentle shaking. Fig. 3c-e shows the quartz glass substrate casted with CPG gel which forms transparent films on drying. The emission property of this film CPG is remains intact. This clearly indicates that these hybrid nano-assemblies are highly processable which is paramount for large area coating.

In conclusion, the preceding results show the design and synthesis of a new coordination polymer gel based on a TPE gelator and Eu(III) ion. Metal coordination provided structural control and transforms the morphology from 1D nanofiber to nanotubes with high mechanical stability. The combined effect of AIE and metal-coordination leads to enhanced and tunable emission in self-assembled gel state. CPGs are highly solution processable and made into transparent films. This new approach of combining AIE and MCIE would provide alternative route for fabrication of luminescent soft functional hybrid materials for solid state lighting and related applications.

Notes and references

∗Molecular Materials Laboratory, Chemistry & Physics of Materials Unit (CPMU), Jawaharlal Nehru Centre for Advanced Scientific Research, Bangalore, India. Email: tmaji@jncasr.ac.in, Tel: +91-8022082826

†We thank Prof. C. N. R. Rao for support and encouragement. Dr. Rajesh Ganapathy for rheological measurements. Selvi, Mrs.Usha for FESEM & TEM measurements. VMS thank CSIR for fellowship.

1 (a) J. W. Steed, *Chem. Soc. Rev*., 2010, **39**, 3686; (b) A. Ajayaghosh, V. K. Praveen, *Acc. Chem. Res.*, 2007, **40**, 644; (c) L. C. Palmer, S. I. Stupp, *Acc. Chem. Res.*, 2008, **41**, 1674; (d) T. Shimizu, M. Masuda, H. Minamikawa, *Chem. Rev.*, 2005, **105**, 1401; (e) J. P. Hill, W. S. Jin, A. Kosaka, T. Fukushima, H. Ichihara, T. Shimomura, K. Ito, T. Hashizume, N. Ishii, T. Aida, *Science* 2004, **304**, 1481; (f) D. Goerl, X. Zhang, F. Würthner, *Angew. Chem. Int. Ed.*, 2012, **51**, 6328; (g) S. H. Seo, J. Y. Chang, G. N. Tew, *Angew. Chem. Int. Ed.*, 2006, **45**, 7526; (h) F. J. M. Hoeben, P. Jonkheijm, E. W. Meijer, A. P. H. J. Schenning, *Chem. Rev.*, 2005, **105**, 1491; (i) G. John, G. Zhu, J. Li and J. S. Dordick, *Angew. Chem. Int. Ed.*, 2006, **45**, 4772.

2 (a) A. Schenning, E. W. Meijer, *Chem. Commun.*, 2005, 3245; (b) A. Ajayaghosh, V. K. Praveen, C. Vijayakumar, *Chem. Soc. Rev.*, 2008, **37**, 109; (c) T. Sendai, S. Biswas, T. Aida, *J. Am. Chem. Soc.*, 2013, **135**, 11509; (d) C. Vijayakumar, V. K. Praveen, A. Ajayaghosh, *Adv. Mater.*, 2009, **21**, 2059; (e) T. Kato, N. Mizoshita, K. Kishimoto, *Angew. Chem. Int. Ed.*, 2006, **45**, 38; (f) P. A. Korevaar, T. F. A. de Greef, E. W. Meijer, *Chem. Mater.*, 2014, **26**, 576; (g) W. Y. Yang, E. Lee, M. Lee, *J. Am. Chem. Soc.*, 2006, **128**, 3484; (h) L. Chen, K. S. Mali, S. R. Puniredd, M. Baumgarten, K. Parvez, W. Pisula, S. De Feyter, K. Müllen, *J. Am. Chem. Soc.*, 2013, **135**, 13531.

3 (a) Y. Hong, J. W. Y. Lam, B. Z. Tang, *Chem. Soc. Rev*., 2011, **40**, 5361; (b) P. -I. Shih, C. -Y. Chuang, C. -H. Chien, E. W. -G. Diau, C. -F. Shu, *Adv. Funct. Mater.*, 2007, **17**, 3141; (c) Q. Chen, D. Zhang, G. Zhang, X. Yang, Y. Feng, Q. Fan, D. Zhu, *Adv. Funct. Mater.*, 2010, **20**, 3244.

4 (a) W. Z. Yuan, P. Lu, S. Chen, J. W. Y. Lam, Z. Wang, Y. Liu, H. S. Kwok, Y. Ma, B. Z. Tang, *Adv. Mater.*, 2010, **22**, 2159; (b) J. Y. Kim, T. Yasuda, Y. S. Yang, C. Adachi, *Adv. Mater.*, 2013, **25**, 2666; (c) Y. Liu, C. Deng, L. Tang, A. Qin, R. Hu, J. Z. Sun, B. Z. Tang, *J. Am. Chem. Soc.*, 2010, **133**, 660.

5 (a) N. B. Shustova, B. D. McCarthy and M. Dinca, *J. Am. Chem. Soc.*, 2011, **133**, 20126; (b) V. M. Suresh, S. Bonakala, S. Roy, S. Balasubramanian and T. K. Maji, *J. Phys. Chem. C* 2014, **118**, 24369; (c) Y. Xu, L. Chen, Z. Guo, A. Nagai and D. Jiang, *J. Am. Chem. Soc.*, 2011, **133**, 17622.

6 S. L. Gould, D. Tranchemontagne, O. M. Yaghi and M. A. Garcia-Garibay, *J. Am. Chem. Soc.*, 2008, **130**, 3246.

7 (a) A. Y. -Y. Tam, V. W. -W. Yam, *Chem. Soc. Rev.*, 2013, **42**, 1540; (b) L. Wang, Y. Liu, Z. Shen, T. Wang and M. Liu, *Chem. Commun.*, 2014, **50**, 15874; (c) H. J. Kim, W. C. Zin, M. Lee, *J. Am. Chem. Soc.*, 2004, **126**, 7009; (d) C. Li, K. Deng, Z. Tang, L. Jiang, *J. Am. Chem. Soc.*, 2010, **132**, 8202; (e) P. Byrne, G. O. Lloyd, L. Applegarth, K. M. Anderson, N. Clarke, J. W. Steed, *New J. Chem.*, 2010, **34**, 2261; (f) J. Zhang, X. Wang, L. He, L. Chen, C. -Y. Su, S. L. James, *New J. Chem.*, 2009, **33**, 1070.

8 (a) Y. Pan, Y. Gao, J. Shi, L. Wang, B. Xu, *J. Mater. Chem.*, 2011, **21**, 6804; (b) Y. Li, A. Y. -Y. Tam, K. M. -C. Wong, W. Li, L. Wu, V. W. -W. Yam, *Chem. Eur. J.*, 2011, **17**, 8048; (c) S. -T. Lam, V. W.-W. Yam, *Chem. Eur. J.*, 2010, **16**, 11588; (d) W. L. Leong, A. Y. -Y. Tam, S. K. Batabyal, L. W. Koh, S. Kasapis, V. W. -W. Yam, J. J. Vittal, *Chem. Commun.*, 2008, 3628.

9 (a) M. -O. M. Piepenbrock, G. O. Lloyd, N. Clarke, J. W. Steed, *Chem. Rev.*, 2010, **110**, 1960; (b) P. Sutar, V. M. Suresh, T. K. Maji, *Chem. Commun.*, 2015, **51**, 9876; (c) O. Roubeau, A. Colin, W. Schmitt, R. Clerac, *Angew. Chem. Int. Ed.*, 2004, **43**, 3283; (d) Y. Liao, L. He, J. Huang, J. Zhang, L. Zhuang, H. Shen, C. -Y. Su, *ACS Appl. Mater. Interfaces*, 2010, **2**, 2333; (e) L. Yang, L. Luo, S. Zhang, X. Su, J. Lan, C. -T. Chen, J. You, *Chem. Commun.*, 2010, **46**, 3938; (f) M. -O. M. Piepenbrock, N. Clarke, J. W. Steed, *Soft Matter* 2011, **7**, 2412; (g) Q. Liu, Y. Wang, W. Li, L. Wu, *Langmuir* 2007, **23**, 8217. (h) O. Kotova, R. Daly, C. M. G. dos Santos, M. Boese, P. E. Kruger, J. J. Boland, T. Gunnlaugsson, *Angew. Chem. Int. Ed.*, 2012, **51**, 7208; (i) Y. Zhang, B. Zhang, Y. Kuang, Y. Gao, J. Shi, X. X. Zhang, B. Xu, *J. Am. Chem. Soc.*, 2013, **135**, 5008; (j) Y. -R. Liu, L. He, J. Zhang, X. Wang, C. -Y. Su, *Chem. Mater.*, 2009, **21**, 557; (k) J. B. Beck, S. J. Rowan, *J. Am. Chem. Soc.*, 2003, **125**, 13922; (l) P. K. Vemula and G. John, *Chem. Commun.*, 2006, 2218.

10 (a) V. M. Suresh, S. J. George and T. K. Maji, *Adv. Funct. Mater.*, 2013, **23**, 5585; (b) V. M. Suresh, S. Chatterjee, R. Modak, V. Tiwari, A. B. Patel, T. K. Kundu and T. K. Maji, *J. Phys. Chem. C,* 2014, **118**, 12241.

11 (a) P. P. Kapadia, L. R. Ditzler, J. Baltrusaitis, D. C. Swenson, A. V. Tivanski, F. C. Pigge, *J. Am. Chem. Soc.*, 2011, **133**, 8490; (b) J. Wang, J. Mei, R. Hu, J. Z. Sun, A. Qin, B. Z. Tang, *J. Am. Chem. Soc.*, 2012, **134**, 9956.

12 W.-H. Yu, C. Chen, P. Hu, B.-Q. Wang, C. Redshaw and K.-Q. Zhao, *Rsc Advances*, 2013, **3**, 14099; (b) W. Z. Yuan, F. Mahtab, Y. Gong, Z.-Q. Yu, P. Lu, Y. Tang, J. W. Y. Lam, C. Zhu, B. Z. Tang, *J. Mater. Chem.* 2012, **22**, 10472.

13 (a) N. N. Adarsh and P. Dastidar, *Cryst. Growth Des.*, 2011, **11**, 328; (b) B. S. Luisi, K. D. Rowland and B. Moulton, *Chem. Commun.*, 2007, 2802.

Table of Contents (TOC)

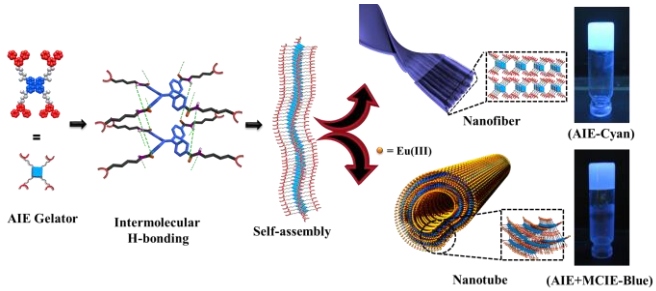

Self-assembly of a rationally designed AIE active LMWG, driven by intermolecular H-bonding form 1D nanostructures which entangled to form micron length nanofibers with strong cyan emission due to AIE property of TPE core. On the other hand, addition of metal ion causes the formation of nanotubular structures with strong blue emission in gel state due to AIE and MCIE.